Particle Production at HERA

A.Grebenyuk

on behalf of the H1 and ZEUS collaborations

DESY
Notkestr. 85, D-22607 Hamburg, Germany
E-mail: anastasia.grebenyuk@desy.de

Results on particle production in deep-inelastic scattering in ep collision at HERA, obtained with the H1 and ZEUS detectors, are presented. The underlying parton dynamics are investigated by looking at the hardness of the transverse momentum distribution of charged particles and comparing the measurements with various Monte Carlo generators using different approaches to simulate the parton cascade. Studies of the scaled momentum distribution for charged hadrons as well as for K^0_S and Λ particles in the current fragmentation region of the Breit frame in the context of hadronisation are presented. The data are compared to models and to next-to-leading order QCD calculations.

1 Charged particle production and parton dynamic

In the region of small x at the HERA collider effects from non-p_T-ordered parton radiation might become visible. Measurements, where in addition to the scattered electron, charged hadrons are measured can be sensitive to the underlying parton dynamics. In [1] it has been proposed that the transverse momentum spectrum of charged particles is sensitive to whether the partons are emitted in a p_T-ordered cascade (DGLAP) or in a unordered way (beyond DGLAP).

We present [2] measurements of the transverse momenta and pseudorapidities of charged particles in different regions of x and Q^2, and compare them to predictions of various Monte Carlo (MC) generators using different approaches to simulate the parton cascade: the RAPGAP generator [3] based on leading-log DGLAP parton showers [4]; the DJANGOH [5] MC which uses the Colour Dipole Model (CDM) [7] as implemented

in ARIADNE [6], and which provides a description of gluon emissions which are similar to that of the BFKL evolution [8]; the CASCADE generator [11] based on the CCFM model [9], which unifies the BFKL and DGLAP approaches and requires angular ordering of the emitted partons w.r.t the proton beam. In the CDM and the CCFM approaches the p_T of the emitted partons in a parton shower is not ordered. All generators use the Lund string model [12] for hadronisation as implemented in PYTHIA [13]. In addition, we use a parameter set tuned by the ALEPH collaboration to fit LEP data [14].

The analysed data set corresponds to an integrated luminosity of $L = 88.64$ pb^{-1}, and the phase space is defined by $5 < Q^2 < 100$ GeV^2, $0.05 < y < 0.6$, $155^\circ < \theta_e < 175^\circ$ and $E_e > 12$ GeV, with θ_e and E_e being the polar angle and energy of the scattered positron, respectively. The data are corrected for detector acceptance, efficiency and resolution effects, as well as for the charged decay products of K^0_S, Λ and for other weakly decaying particles. The measurements of transverse momenta and pseudorapidities of charged particles are presented in the hadronic centre-of-mass system (HCM), i.e. in rest frame of the virtual photon and proton, and labeled as p^*_T and η^*, respectively. All distributions shown are normalised to the total number of DIS events in the analysed phase space.

1.1 Transverse momentum and rapidity distributions of charged particles

The transverse momentum spectra (p^*_T) of charged particles are presented in Fig. 1 for two pseudorapidity intervals: in $1.5 < \eta^* < 4$, where current fragmentation is important, and in the more central region, $0 < \eta^* < 1.5$, where target fragmentation is also playing a role. The DJANGOH predictions, based on the CDM, describes the data fairy well for the whole p^*_T range, whereas RAPGAP is below the data for $p^*_T > 1$ GeV, especially in the central pseudorapidity interval. In contrast, CASCADE is above the data for almost the whole p^*_T range.

The normalised rapidity distributions were measured for $p^*_T < 1$ GeV and for $p^*_T > 1$ GeV, shown separately in Fig. 2. As argued in [1], hadronisation effects should be relevant at small p^*_T, while hard parton radiation should manifest itself in the tail of the p^*_T distribution. To check the sensitivity to hadronisation effects, RAPGAP prediction with default PYTHIA fragmentation parameters and with parameters tuned by ALEPH are shown in Fig. 2. Significant differences between these two models are seen in the soft p^*_T region, while for particles with harder transverse momenta this discrepancy is much smaller. Comparing predictions from generators with different QCD scenarios for parton cascades at large p^*_T, where the influence of the fragmentation is much smaller, but clear differences between the models with different parton cascades are observed.

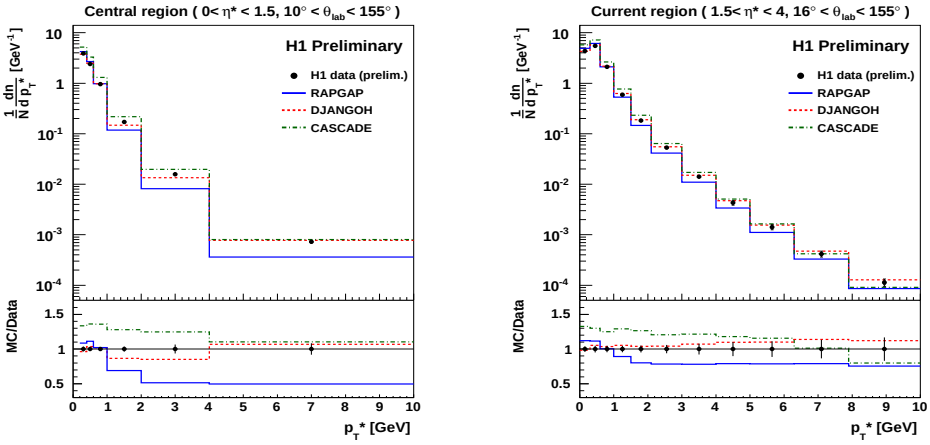

Figure 1: Measured p_T^* spectra of charged particles in the hadronic centre-of-mass system (HCM) in the two pseudorapidity intervals: $0.5 < \eta^* < 1.5$ and $1.5 < \eta^* < 4$ together with RAPGAP, DJANGOH and CASCADE predictions.

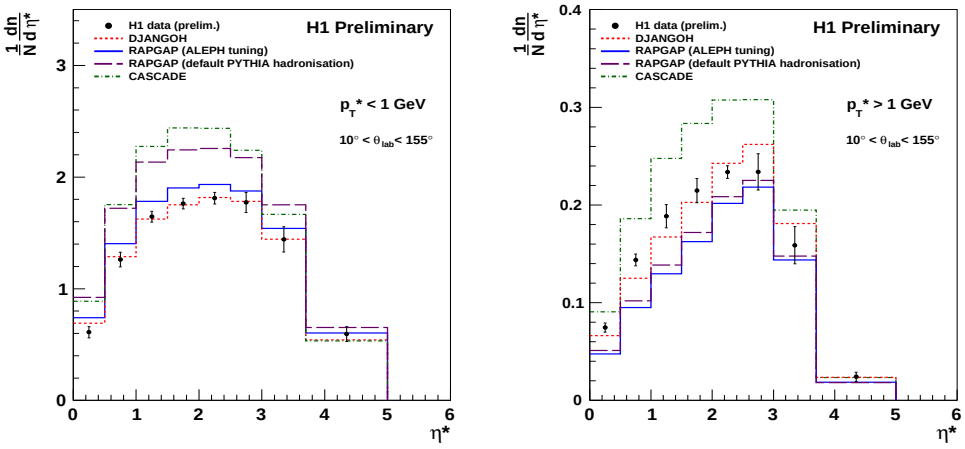

Figure 2: Measured η^* spectra of charged particles in the hadronic centre-of-mass system for $p_T^* < 1$ GeV (left) and for $p_T^* > 1$ GeV (right) together with RAPGAP, DJANGOH and CASCADE predictions. The proton remnant direction is to the left.

The charged particle multiplicity as a function of pseudorapidity in different x and Q^2 bins are shown in Fig. 3 for $p_T^* > 1$ GeV. A significant surplus of hard particles in data over predictions from the DGLAP model RAPGAP at small x and towards the proton remnant is observed. The CASCADE calculations are above the data everywhere, especially at large values of x and Q^2.

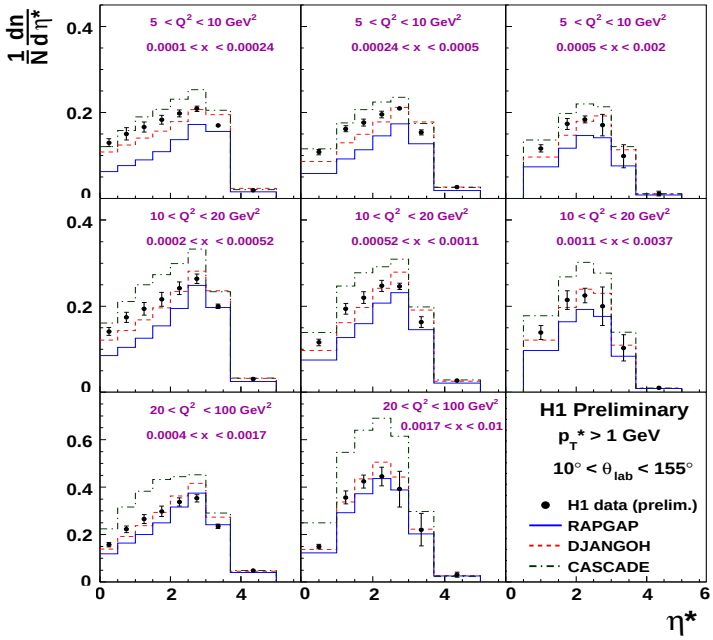

Figure 3: Measured η^* spectra of charged particles in the hadronic centre-of-mass system for $p_T^* > 1$ GeV, for eight intervals of Q^2 and Bjorken-x as indicated on the plot, together with Monte Carlo predictions. The proton remnant direction is to the left.

2 Scaled momentum distributions

ZEUS collaboration investigated production of charged particle as well as K_S^0 and Λ in the current fragmentation region of the Breit frame. Multiplicity distributions are presented as a function of Q^2 per unit of the scaled momentum, $x_p = 2p^{Breit}/Q$. Here, p^{Breit} denotes the momentum of a hadron in the Breit frame.

The aim was to check the universality of the quark fragmentation function and the

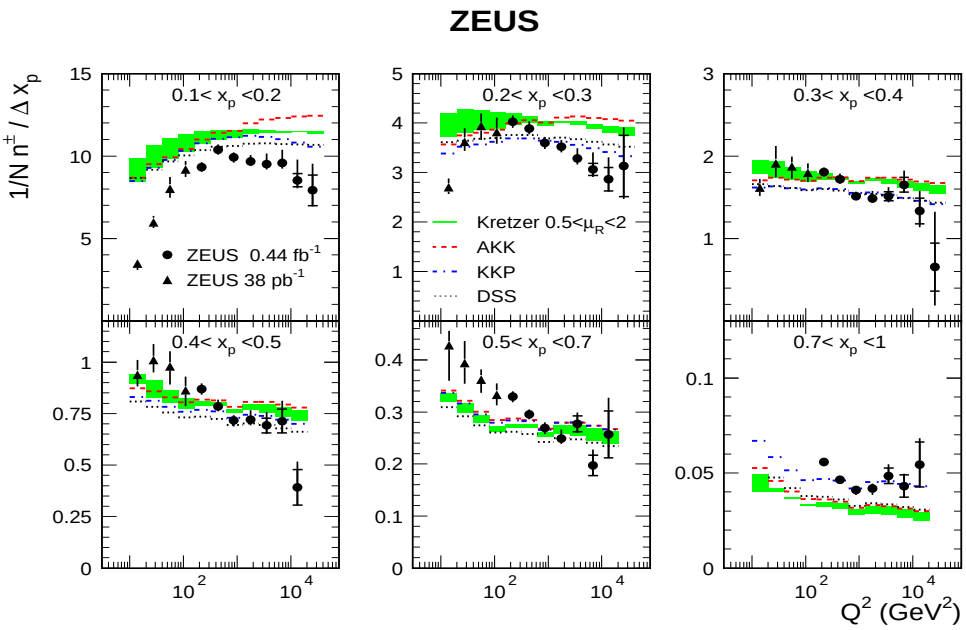

Figure 4: The scaled momentum distributions as a function of Q^2 in different regions of x_p for charged particles together with the predictions of NLO QCD using different fragmentation functions.

factorisation theorem approach used to predict hadron production in different processes. The scaled momentum distributions were compared with next-to-leading order (NLO) QCD calculations. Various fragmentation functions (FFs), obtained from fits to e^+e^- data [15, 16], to e^+e^- and $pp/p\bar{p}$ data [17], or to e^+e^-, $pp/p\bar{p}$ and ep data [18], used in the NLO QCD calculations. All distributions shown are normalized to the total number of DIS events in the analysed phase space.

2.1 Scaled momentum distributions of charged particles

Scaled momentum spectra were measured in the current region in the Breit frame as a function of Q^2 in the kinematic range $160 < Q^2 < 40960$ GeV^2 and $0.002 < x < 0.75$ [20]. The analysed data set corresponds to an integrated luminosity of $L = 0.44$ fb^{-1}. The data are corrected for detector acceptance, efficiency and resolution effects, as well as for the charged decay products of K^0_S, Λ and for other weakly decaying particles.

Results are presented in Fig. 4. Also shown in Fig. 4 are previously published results for $10 < Q^2 < 160$ GeV^2. With increasing Q^2 the phase space for soft gluon radiation gets enlarged, which leads to a rise in the number of soft particles at small x_p and to a decrease in the number of those with high x_p. This scaling violation can be seen for charged particles for large Q^2 values. The data are compared with four NLO QCD predictions using different fragmentation functions [15, 16, 17, 18]. The uncertainties are only illustrated for the calculation of Kretzer [15]. The NLO calculations do not provide a good description of the data and show a different x_p slope, and the scaling violations predicted are not strong enough.

2.2 K^0_S and Λ scaled momentum distributions

Scaled momentum distributions for K^0_S and Λ were measured in the kinematic range $10 < Q^2 < 40000$ GeV^2 and $0.001 < x < 0.75$ [19]. The analysed data set corresponds to an integrated luminosity of $L = 290$ pb^{-1}.

Fig. 5 (left) and Fig. 5 (right) show the scaled momentum spectra, as a function of Q^2 in different regions of x_p, respectively. The NLO QCD predictions using two different FFs describe the data only in certain region of the phase space. For the AKK+CYCLOPS calculations it is limited to $0.6 < x_p < 1$, whereas the DSS calculations describe the K^0_S data adequately, except for regions of low x_p and Q^2. Together with the NLO QCD calculations predictions from the colour dipole model as implemented in the MC ARIADNE and from the leading-log parton shower MC LEPTO [10] are shown for K^0_S and Λ. Both predictions give a reasonable description of the data over almost the whole phase space.

3 Conclusion

Production of the charged particles has been studied in deep-inelastic scattering at HERA. The measurements of the transverse momentum and pseudorapidity of charged particles at low values of x show the importance of a parton emissions unordered in transverse momentum. A QCD model, which includes such mechanism, as the BFKL-like colour dipole model is best in the description of the data, whereas a model generating emissions according to the DGLAP approach undershoots the data at large p^*_T and low η^* (in the proton remnant direction). It is also shown that hadronisation effects are important at low p^*_T, while parton radiation manifest itself in a hard tail of the transverse momentum distribution. Scaling violations are clearly observed in the measurements

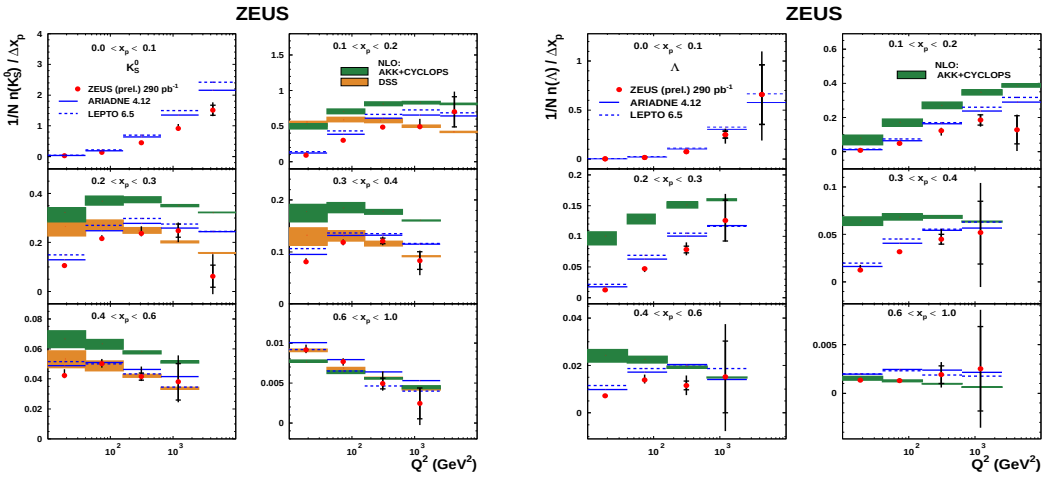

Figure 5: The scaled momentum distributions as a function of Q^2 in different regions of x_p for K^0_S (left) and Λ (right) together with the predictions of NLO QCD and LO QCD models implemented in Monte Carlo programs.

of scaled momentum distribution for all charged particles as well for both K^0_S and Λ. Next-to-leading order QCD calculations based on different fragmentation functions can describe the data only in some regions of x_p. A better description of the data for K^0_S and Λ production in most parts of the phase space is provided by the predictions based on models which include LO matrix elements and parton showers as implemented in the ARIADNE and LEPTO programs.

References

[Slides] http://indico.cern.ch/getFile.py/access?contribId=64&resId=0&materialId=slides&confId=139914

[1] M. Kuhlen, Phys. Lett. B **382** (1996) 441.

[2] H1 Preliminary DIS2011, H1prelim-11-035

[3] H. Jung, Comp. Phys. Commun. 86(1995) 147

[4] V. Gribov and V. Lipatov, Sov. J. Nucl. Phys. **15** (1972) and 675;
V. Lipatov, Sov. J. Nucl. Phys. **20** (1975) 94;

G. Altarelli and G. Parisi, Nucl. Phys. B **126** (1977) 298;
Y. Dokshitzer, Sov. Phys. JETP **46** (1977) 641;

[5] K. Charchula, G.A. Schuler, H. Spiesberger, Comp. Phys. Commun. **81** (1994) 381

[6] L. Lönnblad, ARIADNE 4.10. Comput. Phys. Commun. **71** (1992) 15.

[7] B. Andersson *et al.*, Z.Phys. C 43 (1989) 625,
L. Lönnblad, Comput. Phys. Commun. **71** (1992) 15.

[8] E. Kuraev, V. Lipatov and V. Fadin, Sov. Phys. JETP **44** (1976) 443;
E. Kuraev, V. Lipatov and V. Fadin, Sov. Phys. JETP **45** (1977) 199;
Y. Balitsky and V. Lipatov, Sov. J. Nucl. Phys. **28** (1978) 822;

[9] M. Ciafaloni, Nucl. Phys. **296** (1988) 49;
M. Catani, F. Fiorani and G. Marchesini, Phys. Lett. **234** (1990) 339;
M. Catani, F. Fiorani and G. Marchesini, Nucl. Phys. **336** (1990) 18.

[10] G. Ingelman *et al.*, Comput. Phys. Commun. **101** (1997) 108.

[11] H. Jung, Comp. Phys. Commun. 143 (2002) 100

[12] B. Andersson, G. Gustafson, G. Ingelman and T. Sjostrand,
Phys. Rept. **97** (1983) 31

[13] T. Sjostrand *et al.*, PYTHIA V6.1, Comp. Phys. Commun. **135** (2001) 238.

[14] I. G. Knowles *et al.*, Workshop on Physics at LEP2, v.2, Geneva, Switzerland, 2 - 3 Nov 1995, p.103

[15] S. Kretzer, Phys.Rev. D 62, (2000) 054001.

[16] B.A. Kniehl, G. Kramer and B.Pötter, Phys.Rev. Lett. **85**, (2000) 5288.

[17] S. Albino, B.A. Kniehl and G. Kramer, Nucl. Phys. B **725** (2005) 181;
S. Albino, B.A. Kniehl and G. Kramer, Nucl. Phys. B **803** (2008) 42.

[18] D.De Florian, R. Sassot and M. Stratmann, Phys. Rev. D **75** (2007) 114010,
D.De Florian, R. Sassot and M. Stratmann, Phys. Rev. D **76** (2007) 074033.

[19] ZEUS Preliminary ICHEP2010, ZEUS-prel-10-013

[20] H. Abramowicz *et al.* [ZEUS Collaboration], JHEP **11** (2010) 1.